TYPE II SUPERNOVAE AT HIGH REDSHIFTS

N.N. CHUGAI[1], S.I. BLINNIKOV[2], P. LUNDQVIST[3]
[1]*Institute of Astronomy RAS, Moscow, Russia*
[2]*Institute for Theoretical and Experimental Physics, Moscow, Russia*
[3] *Stockholm Observatory, Saltsjöbaden, Sweden*

ABSTRACT. A hydro code coupled with radiation transfer was applied to produce monochromatic light curves of two models of type II supernovae (SN II) simulating SN II-P and SN IIb (SN 1993J-like). We then used these template light curves to evaluate the possibility of detecting SNe II at different redshifts. With a 5 hour exposure at VLT/FORS the SN II-P model may be detected at $z = 1$. However, since our model of SN II-P is underluminous at early phase ($t < 10$ days) by ≈ 1.5 mag a detection at $z = 2$ is quite plausible. SN IIb can be detected as far as at $z = 4$. For 100% detection efficiency up to $z = 2$ one expects to find roughly 1 SN II yr^{-1} arcmin^{-2}.

1. Introduction

Type II supernovae trace closely the overall star formation process and metal enrichment of galaxies and intergalactic space. Therefore, the observation of high z SNe II would be a complementary test of cosmic evolution models, being developed intensively during the latest several years. The depth of imaging of distant sources reached recently by HST, Keck I and II, and also by VLT raises an exciting possibility of observations of SNe II at $z > 1$. Due to high UV/optical luminosity after the shock breakout some of SNe II may be luminous enough to be detected at extremely high z, possibly even at pre-galactic epoch $z \geq 10$. By some reason (e.g., lower metallicity) at high z we may find also different, possibly even more luminous, types of collapse events (e.g., like SN 1998bw).

An obvious prerequisite for high redshift study of SNe II is a set of template rest-frame monochromatic UV/optical light curves for different subtypes of SNe II. Unfortunately, a complete sample of template observed light curves is not available at present. Even for the best observed SN 1987A and SN 1993J, the early epoch following the shock wave breakout is missing. We note in this context that these supernovae, both representing rare subtypes, were used for calculations of rate–magnitude relation by Jørgensen et al. (1997).

Alternatively, we may rely on theoretical light curves. However, not until now realistic modeling of SN II spectra has become possible. The hydro-code we have used to do this is coupled with radiation transfer (Blinnikov and Bartunov 1993, Blinnikov et al. 1998). It permits us to produce supernova models, which we then use to recover the early UV/optical behavior of SNe II. The creation of a set of template light curves for different kinds of SNe II (viz. SN II-P, SN II-L, SN IIn) requires extensive modeling. This is under way (Chugai et al. 1999).

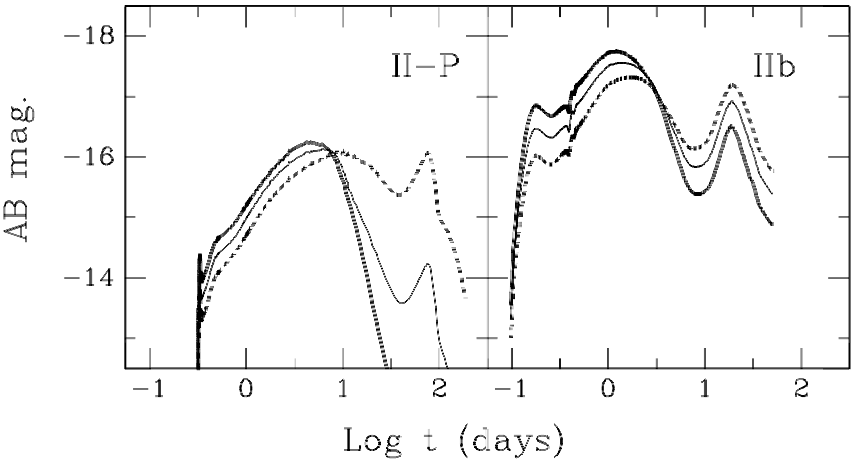

Fig. 1. Light curves of SN II models. Absolute monochromatic AB magnitude is defined following Oke & Gunn (1983) with wavelengths equal to the effective wavelengths of U band (thick solid line), B (thin solid) and V (dotted).

Here we report on preliminary results of the evaluation of detection feasibility for high redshift SNe II on the basis of two models: SN II-P and a low mass SN 1993J-like event, referred to as SN IIb (Woosley et al. 1987). We do not consider here models of SN II-L and SN IIn, which is still a subject of study. We estimate also the frequency of SN II events for different modes of cosmic star formation rate and give an assessment of SN II detection in the search with VLT. In this preliminary study we have not included dust extinction. This will be done in our fuller analysis (Chugai et al. 1999).

2. Models and monochromatic light curves

If the wind around pre-SN is of low density, the light curve of SN II is determined only by the ejected mass (M), kinetic energy (E), pre-SN radius (R_0), density structure and composition of the hydrogen envelope. The bulk of type II supernovae is SN II-P. This class is simulated here by a model with parameters $R_0 = 300\ R_\odot$, $M = 14\ M_\odot$, $E = 1.0 \times 10^{51}$ ergs. The density distribution in the pre-SN is that of SN 1987A rescaled to a radius of 300 $R_\odot$. The underlying model is 14E1 used by Shigeyama & Nomoto (1990). The second model represents low mass SN II or SN IIb with $R_0 = 300\ R_\odot$, $M = 2.5\ M_\odot$and $E = 1.3 \times 10^{51}$ ergs. This is the model 13C of Woosley et al. (1994) which was used to simulate SN 1993J. Although this is a relatively rare subclass, we have chosen to include a model of the well studied SN 1993J to show the effect of the relatively strong initial UV/optical peak, which is characteristic of low mass extended pre-SN II. In this sense the model SN IIb may be a good proxy for SN II-L, as well as SN IIn, which both have rather extended envelopes presumably related to a strong stellar wind.

The absolute monochromatic light curves calculated at wavelengths corresponding

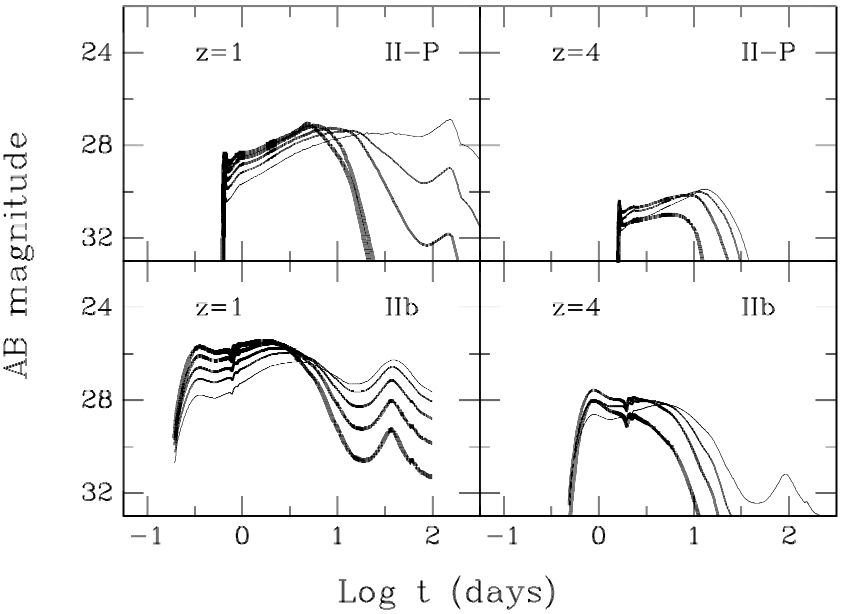

Fig. 2. Monochromatic BVRIJ light curves for SN II models at $z = 1$ and $z = 4$. From B band (thick line) through J band (thin line) line thickness decreases.

to the effective wavelengths in the UBV bands for both models are shown in Fig. 1. SN IIb are ≈ 1.8 mag brighter in UBV than SN II-P at first maximum light between 1–10 day. This reflects the different density structures of the outer layers of these pre-SN models. It should be emphasized that our SN II-P model does not represent an average SN II-P in detail. Moreover, it is somewhat underluminous (by ~ 1.5 mag) in the UBV bands at the initial phase 1–10 days compared to observations. For example, SN 1988A, a supernova of type II-P subclass with a clearly observed early rise, has an initial maximum at the level of $M_V = -17.7$ mag (Turatto et al. 1993). This is 1.6 mag brighter than in our model ($M_V = -16.1$ mag). The choice of an adequate model for SN II-P requires the reconstruction of the pre-SN II-P on the basis of a fit to UBV light curves and photospheric velocity evolution of representative SN II-P.

At redshifts $z = 1$ and $z = 4$ the models produce the BVRIJ light curves shown in Fig. 2. The Lyman continuum absorption in the host galaxy and the integrated absorption by Lα forest have been taken into account, the latter following the recipe of Press, Rybicky & Schneider (1993). Note that hydrogen absorption is responsible for the suppression of the B flux at $z = 4$ (Fig. 2). It is remarkable that, while the light curves are different for different models and bands, the maxima of the R, I, and J magnitudes at $z \approx 4$ are quite similar. Amazingly enough, the light curve of the SN II-P model in the V band becomes narrow at high z in spite of time dilation. Such a behavior stems from the decrease of the rest frame light curve width as wavelength becomes shorter.

The most striking property of all the light curves of SN II at various z is the fast

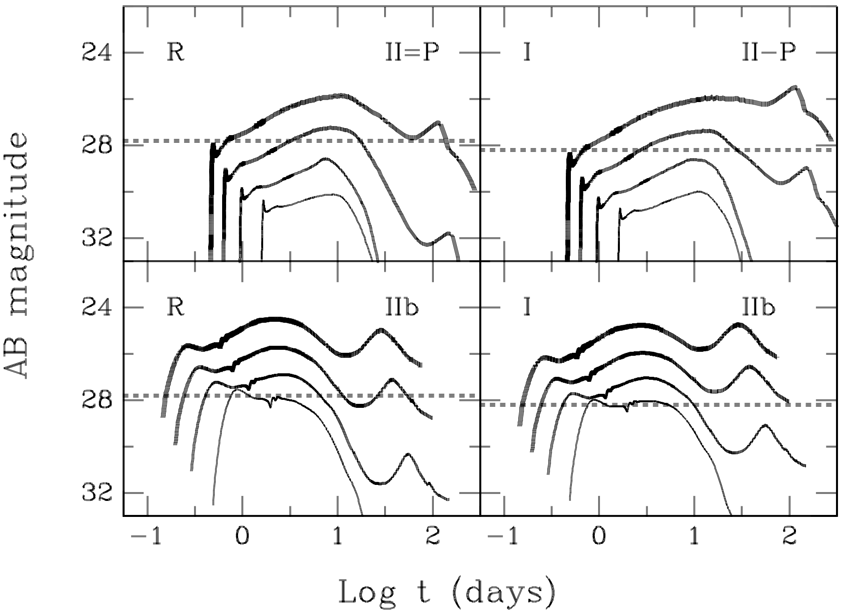

Fig. 3. Monochromatic R and I light curves of SN II models at different redshifts. Model SN II-P and model SN IIb light curves are shown for z equal to 0.5, 1, 2, 4 with line thickness decreasing from $z = 0.5$ (thick line) through $z = 4$ (thin line). The detection limits for 5 hour exposure at VLT/FORS are shown by dotted lines.

early rise ($t_\mathrm{r} \approx 1$ day) to maximum (or nearly maximum) luminosity. This property, very specific for SNe II, is unlike the light curves of SN Ia and SN Ib, which are characterized by a broad rise to maximum ($t_\mathrm{r} > 20$ days at $z \geq 1$). The latter is demonstrated by the secondary maximum at $t > 30$ days in the model SN IIb, which is very similar to the main maximum in SN Ib and SN Ia models. The shape of light curves at the initial phase may be a crucial signature for the identification of high redshift SN II events.

3. Detectability by VLT and rate of events

With a 5 hour exposure on VLT/FORS the limiting magnitudes in the V, R, and I bands are 27.5 (S/N = 6.2), 27.8 (S/N = 6.7), and 28.2 (S/N = 6.4), respectively, assuming an airmass of 1.5, and a seeing of 0."8. For such an exposure, our model SN II-P can be detected by VLT in the R and I bands at $z \approx 1$ (Fig. 3). However, since the detection limit of SN II-P is most likely underestimated because our SN II-P model is underluminous by ~ 1.5 mag at the initial phase $t \geq 10$ days, SN II-P can probably be seen by VLT at least up to $z = 2$. In the case of SNe IIb a secure detection is guaranteed at $z = 2$ and they may be observed even up to $z = 4$ in both the R and I bands (Fig. 3).

There are clear indications that supernovae of subtypes SN II-L (e.g., SN 1979C) and SN IIn (e.g., SN 1994W) produce strong initial UV/optical peak ($M_{B,V} \sim -(18-19)$.

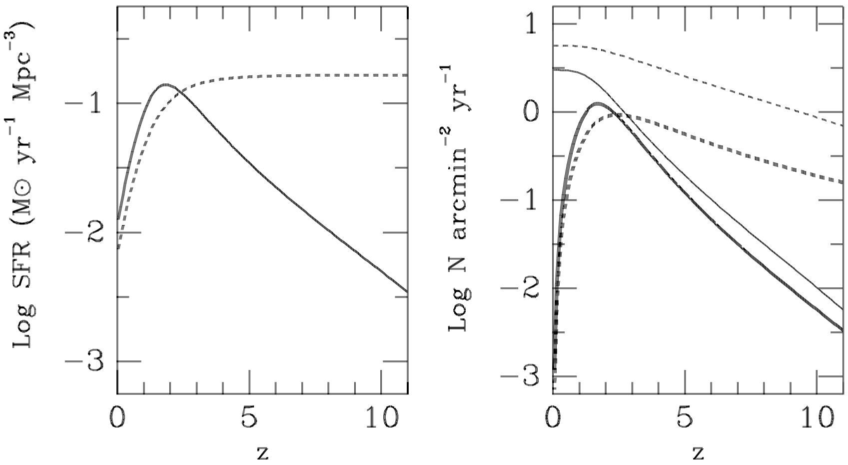

Fig. 4. Star formation rate and rates of core collapse supernovae. Left panel shows two types of star formation evolution: late (solid line) and early (dotted), while on the right panel shown are corresponding "observed" rate of supernovae per unit of z (thick lines) and cumulative rate (thin lines).

This is related presumably to the presence of an extended envelope and/or wind, which are rarefied enough for the shock wave energy to escape avoiding severe adiabatic loss. We predict that both these kinds of SNe II could be well observed at redshifts $z \geq 4$. However, this claim requires a confirmation in light curve computations.

The observing rate of core-collapse supernovae at some z is determined by the co-moving star formation rate (SFR), the initial mass function (IMF), the minimum initial mass of stars producing supernovae, M_2, and the cosmological model adopted. A reasonable estimate of the total rate of core collapse supernovae may be obtained assuming that all stars with the present day ratio of stellar density to critical, $\Omega_{\rm s}$, were born instantly at some characteristic epoch $z = z_{\rm s}$. Then adopting flat cosmology (i.e., $\Omega = 1$) one gets the observing rate

$$\dot{N} = 6c^3\Omega_{\rm s}G^{-1}(dN_{\rm cc}/dm)[1 - 1/(1+z_{\rm s})^{1/2}]^2 \approx 60[1 - 1/(1+z_{\rm s})^{1/2}]^2 \quad ({\rm s}^{-1}). \qquad (1)$$

We adopt $\Omega_{\rm s} = 0.0042$ (Fukugita, Hogan & Peebles 1996), and the number of core collapse supernovae per one solar mass converted into stars, $dN_{\rm cc}/dm \approx 0.012\ {M_\odot}^{-1}$. This value is obtained for $M_2 = 10M_\odot$, a Salpeter IMF with $\alpha = 2.35$, $M_{\rm min} = 0.3M_\odot$, $M_{\rm max} = 100\ M_\odot$, and a returned (into gas) mass fraction of $R = 0.4$. Assuming the star formation epoch was $z_{\rm s} = 3$, we estimate 15 core collapse supernovae per second, or 4.5×10^8 SN yr^{-1}. The rate increases when the star formation epoch is shifted further to the past.

For the more general case of flat cosmology ($\Omega_{\rm M} + \Omega_\Lambda = 1$) with $\Omega_{\rm M} = 0.3$, $H_0 = 65$ km s^{-1} Mpc^{-1} and two different SFR evolution laws (late and early star formation starting at $z = 18$, Fig. 4) the rate per unit of z and cumulative rate $N(> z)$ is shown in Fig. 4. The total cumulative rate is ≈ 3 SN yr^{-1} arcmin^{-2} and ≈ 5.6 SN yr^{-1} arcmin^{-2}

for late and early star formation, respectively, while medians of the rate vs. redshift distribution are 2.7 and 4.5, respectively.

Keeping in mind that SNe II contribute 80% to all core collapse supernova events, we then expect to observe roughly ≈ 1 SN II yr^{-1} arcmin^{-2} at $z \leq 2$ provided the detection efficiency is close to 100%.

The search and identification strategy for SNe II with typical maximum magnitudes around 26-27 should exploit specific shapes of light curves and color evolution of SNe II at high z in V, R, and I. An interesting approach may be based on the sudden appearance at time scale ~ 1 day. This prompts an observing strategy for SN II detection using two images separated by the time interval (Δt), which must be short enough to catch SNe II using its fast appearance, and yet long enough to pick up as large as possible number of events, say $\Delta t \approx 10$ days. Given two deep exposures separated by 10 days and assuming the rate 1 SN II yr^{-1} arcmin^{-2} we should then find on average 1.3 SNe II in the field of view of FORS ($6.8' \times 6.8'$). In the case of VIMOS with the field $14' \times 14'$ we expect to detect in a similar observing situation around 5 SNe II.

Acknowledgements

We thank Ken Nomoto and Stan Woosley for the presupernova models and for support. This research was also supported by the Russian Foundation for Fundamental Research (96-02-19756 and 98-02-16404), the International Science & Technology Center 97-370, and by the Royal Swedish Academy of Sciences. P.L. acknowledges further support from the Swedish Natural Science Research Council.

References

Blinnikov, S.I., Bartunov, O.S.: 1993, *Astron. Astrophys.* **273**, 106

Blinnikov, S.I., Eastman, R., Bartunov, O.S., Popolitov, V.A., Woosley, S.E.: 1998, *Astrophys. J.* **496**, 454

Chugai, N.N., Blinnikov, S.I., Lundqvist, P., Woosley, S.E.: 1999, in preparation.

Fukugita, M., Hogan, C.J., Peebles, P.J.E.: 1996, *Nature* **381**, 489

Jørgensen, H.E., Lipunov, V.M., Postnov, K.A., Prokhorov M.E.: 1997, *Astrophys. J.* **486**, 110

Oke, J.B., Gunn, J.E.: 1983, *Astrophys. J.* **266**, 713

Press, W.H., Rybicki, J.B., Schneider, D.P.: 1993, *Astrophys. J.* **414**, 64

Shigeyama, T., Nomoto, K.: 1990, *Astrophys. J.* **360**, 242

Turatto, M., Cappellaro, E., Benetti, S., Danziger, J.: *Mon. Not. R. Astr. Soc.* **265**, 471

Woosley, S. E., Pinto, P. A., Martin, P. G., Weaver, T. A.: 1987, *Astrophys. J.* **318**, 664

Woosley, S. E., Eastman, R. G., Weaver, T. A., Pinto, P. A.: 1994, *Astrophys. J.* **429**, 300